Photocatalytic degradation of selected anticancer drugs and identification of their transformation products in water by liquid chromatography-high resolution mass spectrometry

Photocatalytic degradation of selected anticancer drugs and identification of their transformation products in water by liquid chromatography-high resolution mass spectrometry

P. Calza[(1)], C. Medana[(2)], M. Sarro[(1)], V. Rosato[(1)], R. Aigotti[(2)], C. Baiocchi[(2)], C. Minero[(1)]

[1] *Department of Chemistry, University of Turin. Via P. Giuria 5, 10125 Torino, Italy*

[2] *Department of Molecular Biotechnology and Health Sciences, University of Turin. Via P. Giuria 5, 10125 Torino, Italy*

**corresponding author. Phone: +390116705268; fax: +390112365241; e-mail: paola.calza@unito.it*

Abstract

A study on the fate of two antineoplastic drugs, methotrexate and doxorubicin, in the aquatic environment is presented. The investigation involved a study of their decomposition under dark experiments, homogeneous photolysis and heterogeneous photocatalysis using titanium dioxide, the identification of intermediate compounds, as well as the assessment of acute toxicity over time. The analysis were carried out using LC (ESI positive mode) coupled with LTQ-Orbitrap analyser; accurate mass-to-charge ratios of parent ions were reported with inaccuracy below 10 mmu, which guarantee the correct assignment of their molecular formula in all cases, while their MS^2 and MS^3 spectra showed several structural-diagnostic ions that allowed to characterize the different transformation products and to discriminate the isobaric species.

Fourteen and eight main species were identified subsequently to doxorubicin or methotrexate transformation. The major transformation processes for doxorubicin involved (poli)hydroxylation and/or oxidation of the molecule, or the detachment of the sugar moiety. Methotrexate transformation involved decarboxylation or the molecule cleavage.

Acute toxicity measurements showed that not only the two drugs exhibit high toxicity, but also their initial transformation products are highly toxic.

Keywords: HRMS, TiO_2, doxorubicin, methotrexate, emerging pollutants, toxicity

Introduction

Pharmaceuticals have become a major group of emerging contaminants as widespread pollutants of surface water, groundwater and drinking water [1-4]. Among them, anticancer drugs are of great importance, owing to their cytotoxicity, mutagenesis and genotoxicity. Therefore, it is crucial to monitor their presence in the environment and to extend the investigation to their transformation products (TPs), as they could contribute to the biotoxic and mutagenic potential [5].

The number of studies investigating cytostatic pharmaceuticals in water samples is limited, probably due to their presence at traces level (ng/L and below) and to their further transformation into other products [5]. Little information is likewise available on the transformation products of these drugs, although some human metabolite and biodegradation products have been already monitored [6].

Liquid chromatography is the primary separation technique for the analysis of antineoplastic drugs [7-11]. Trace level analysis requires high sensibility, specificity and accuracy, achievable by using LC/MS. Mass spectrometry is the most selective technique to identify unknown compounds and, using ESI-MS, it is possible to obtain structurally significant fragmentation ions [12--17].

With this in mind, in a previous work we have investigated the transformation of cyclofosfamide and mitomycin C [18], while in this work we focus on doxorubicin and methotrexate, whose presence was already documented in hospital effluents [17,19] or surface waters [20]. Though, only few studies investigate their biotic or abiotic transformation [21-23].

We aimed to monitor the fate of the selected drugs through a combined evaluation of their photostability, identification of TPs and assessment of their toxicity. Photo-induced reactions are certainly known to play a key role among the abiotic transformation; for such, the disappearance of the two substances and the formation of TPs have been evaluated under UV-A light in ultrapure water or after addition of TiO_2. Heterogeneous photocatalysis is indeed a widely used method not only to achieve the decontamination of aquatic systems [24-27], but also to simulate the transformation processes occurring in the environment. This approach was successfully used in previous studies and permitted to identify several TPs, alongside the parent compounds, in water samples [28-30].

Degradation products were characterized by multiple stage mass spectrometry, using a high resolution ion trap (LTQ-Orbitrap) in order to confirm the elemental composition, together with high resolution MS^n

detection, which provides diagnostic identification and characterization of unknown transformation products.

The future application of the present work could be the more complete analysis of pollution of water (wastewater, surface or groundwater samples) with the extension of the analytes scenario to the products of degradation of anticancer drugs.

2. EXPERIMENTAL

2.1. Material and reagents

Experiments were carried out using TiO_2 Degussa P25 as the photocatalyst. TiO_2 powder was irradiated and washed with distilled water until no signal due to chloride, sulphate or sodium ions could be detected by ion chromatography, in order to avoid possible interference from ions adsorbed on the photocatalyst.

Doxorubicin and methotrexate were purchased from Aldrich and used as received. HPLC grade water was from MilliQ System Academic (Waters, Millipore). HPLC grade methanol (BDH) and acetonitrile (Aldrich) were filtered through a 0.45 μm filter before use. Reagent grade formic acid was from Fluka Chemie (Sigma).

2.2. Irradiation procedures

The irradiation experiments were carried out in Pyrex glass cells, filled with 5 ml of drug solution (15 mg/L) or of a suspension containing the drug (15 mg/L) and TiO_2 (200 mg/L). Samples were subjected to different irradiation times (ranging from 2 min to 4 h), using a Philips TLK/05 lamp 40 Watt with maximum emission at 360 nm. The temperature reached during irradiation was 26° C. After illumination, the entire content of each cell was filtered through a 0.45 μm filter and then analyzed.

2.3. Analytical procedures

All samples were analyzed by HPLC/HRMS. The chromatographic separations, monitored using an MS analyzer, were run on a Phenomenex Luna 150 × 2.1 mm, using an Ultimate 3000 HPLC instrument (Dionex, Milan, Italy). Injection volume was 20 µL and flow rate 200 µL/min. Gradient mobile phase composition was adopted: 5/95 to 100/0 in 40 min methanol/formic acid 0.05 % in water when run on ESI positive mode or acetonitrile/ammonium acetate 0.1 mM in the negative mode.

A LTQ Orbitrap mass spectrometer (Thermo Scientific, Bremen, Germany) equipped with an atmospheric pressure interface and an ESI ion source was used. The LC column effluent was delivered into the ion source using nitrogen as both sheath and auxiliary gas. The tuning parameters adopted for the ESI source were: capillary voltage 37.00 V, tube lens 65 V. The source voltage was set to 3.5 kV. The heated capillary temperature was maintained at 275°C. The acquisition method used was optimized beforehand in the tuning sections for the parent compound (capillary, magnetic lenses and collimating octapole voltages) to achieve maximum sensitivity. Mass accuracy of recorded ions (vs calculated) was ± 10 millimass units (mmu) (without internal calibration).

Analyses were run using full MS (50-1000 *m/z* range), MS^2 and MS^3 acquisition in the positive ion mode, with a resolution of 30000 in FTMS mode. The ions submitted to MS^n acquisition were chosen on the base of full MS spectra abundance without using automatic dependent scan. Collision energy was set to 35 (arbitrary units) for all of the MS^n acquisition methods. MS^n acquisition range was between the values of ion trap cut-off and *m/z* of the fragmented ion. Xcalibur (Thermo Scientific, Bremen, Germany) software was used both for acquisition and for elaboration.

2.4. Toxicity Measurements

The toxicity of samples collected at different irradiation times was evaluated with a Microtox Model 500 Toxicity Analyzer (Milan, Italy). Acute toxicity was evaluated with a bioluminescence inhibition assay using the marine bacterium *Vibrio fischeri* by monitoring changes in the natural emission of the

luminescent bacteria when challenged with toxic compounds. Freeze-dried bacteria, reconstitution solution, diluent (2% NaCl) and an adjustment solution (non-toxic 22% sodium chloride) were obtained from Azur (Milan, Italy). Samples were tested in a medium containing 2% sodium chloride, in five dilutions, and luminescence was recorded after 5, 15 and 30 min of incubation at 15^{o} C; no substantial differences were found between the three contact times, for which we report the results related to 5 minutes of contact. Inhibition of luminescence, compared with a toxic-free control to give the percentage inhibition, was calculated following the established protocol using the Microtox calculation program.

3. RESULTS AND DISCUSSION

3.1. Drugs degradation under homogeneous and heterogeneous photocatalysis

Experiments were run in ESI positive mode, which appeared to be more sensitive and suitable both for the parent compound and for most of the photogenerated products. Figure 1 shows the disappearance of doxorubicin (top) and methotrexate (bottom) as a function of irradiation time under direct photolysis or in the presence of TiO_2. The process of photolysis in ultrapure water promoted a partial drugs degradation as within 1 h of irradiation, almost 60% of methotrexate and 10% of doxorubicin disappeared. TiO_2 addition endorsed a fast degradation and both drugs were efficiently degraded ($t_{1/2}$ 3 and 2 min for doxorubicin and methotrexate, respectively) and completely disappeared within 30 min of irradiation.

Formation of transformation products (TPs) was followed, too. TPs were characterized by assessing the kinetics of formation/disappearance and their MS^n spectra. For each organic compound the structure was assumed on the basis of information derived from high resolution spectra of MS^2 and MS^3 compared with MS^n parent spectra.

3.2. Drugs MS-MS analysis

MS^n study allowed to obtain information useful to identify unknown transformation products formed through drugs degradation. The product ions generated from protonated molecular ions of doxorubicin and methotrexate are collected in Figure2. MS^n fragments identification was confirmed by the high resolution study of neutral losses.

In MS^2 doxorubicin spectrum, several product ions were detected and, in particular, two structural diagnostic ions were evidenced: the product ion at 397.0923 *m/z*, formed from the loss of the sugar moiety and the ion at 321.0764 *m/z*, due to the detachment of the side chain.

Methotrexate MS^2 spectrum showed 308.1261 *m/z* as base peak, formed through succinic amino acid molecule loss. MS^3 fragmentation generated two product ions at 134.0546 and 175.0659 *m/z*, both involving the molecule breaking of middle C-N bond.

3.3. Structural characterization of doxorubicin intermediate compounds

Experiments conducted in the dark did not reveal the formation of any TPs, while direct photolysis showed the formation of eight TPs, whose evolution profiles are collected in Figure S1. All TPs identified through a direct photolysis process were identified after addition of TiO_2, too. Furthermore, six new TPs were formed through heterogeneous photocatalysis, many of which in the form of structural isomers; TPs are all collected in Figure 3. Proposed elemental composition, as well as retention times, are reported in Table 1.

These derivatives can be grouped into two classes: TPs resulting from (poli)hydroxylation and/or oxidation of the molecule (from **D-1** to **D-11**), and the products resulting from the detachment of the sugar moiety (from **D-12** to **D-14**).

Two isobaric species with $[M+H]^+$ 560.1755 and empirical formula $C_{27}H_{30}O_{12}N$ were formed and attributed to monohydroxylated doxorubicin (named **D-1** and **D-2**). For **D-2**, MS^2 spectrum exhibited three key fragments at 379.0871, 361.0719 and 321.0764 *m/z*, all attributable to the detachment of hydroxylated sugar molecule. Conversely, all MS^2 product ions formed from **D-1** were well matched with an hydroxylation involving the other portion of the molecule, reasonably occurring on the aromatic ring. The assumed fragmentation pattern is reported in Figure 4.

Three species with $[M+H]^+$ 576.1710, attributable to dihydroxyl-derivatives, were detected (named **D-3** to **D-5**). **D-5** exhibited two structural diagnostic ions at 379.0871 and 361.0719 *m/z*, attributable to the

detachment of dihydroxylated sugar (see Figure 5). Conversely, in **D-3** and **D-4** the product ion at 429.0822 *m/z* put forward to place both OH groups in the other part of the molecule; for **D-3** the structural diagnostic ion at 337.0712 *m/z* allowed to hypothesize that one (of the two) OH groups lies on the aromatic ring, whereas for **D-4** the favored consecutive loss of water molecules, with the formation of the ion 540.1498 *m/z*, was well-matched with a dihydroxylation involving the hexacycle.

TPs named **D**-**6** to **D**-**10**, based on their empirical formulas, can be attributed to doxorubicin oxidized products.

Four different species at 558.1953 *m/z* were formed and attributed to hydroxylated/oxidized derivatives (named **D-6** to **D-9**).

Key product ions formation permitted to distinguish the different sites for oxidation and hydroxylation on the four isobaric species (see Figure S2). **D-7** MS^2 spectrum exhibited 429.0820 as key fragmentation ion, so suggesting that hydroxylation involved the aromatic ring, while oxidation occurred on the aminosugar moiety. Conversely, for **D-6** the MS^2 product ions at 429.0825 and 411.0723 *m/z* were attributable to the loss of the sugar moiety and the subsequent dehydration of the species obtained, so implying that oxidation but not hydroxylation involved the aminosugar. For **D-8**, the most abundant peak and structural diagnostic ion was 365.0664 *m/z*, formed through the concerted loss of formic acid and sugar molecule, so allowing to set the oxidation site on the methyl group. Confirm also arose from the MS^2 product ion at 321.0759 *m/z*, involving the combined loss of hydrogen peroxide, glyoxal and aminosugar.

Concerning **D-9**, the second most abundant MS^2 ion product was 441.1185 *m/z*, formed through a loss of $C_4H_7O_3N$ following to the breakage of the oxidated and hydroxyled aminosugar moiety. Confirm arose from the presence of the ions at 423.1075 and 405.0973 *m/z*, derived from the same loss than one or two water molecules. The ion at 514.1356 *m/z* could be formed by hydroxylated/oxidated aminosugar ring contraction with the loss of acetaldehyde (see Figure S2 in supplementary material).

By analyzing the species at 542.1695 *m/z* (named **D**-**10**), MS^2 spectrum showed all typical losses occurring on doxorubicin following the detachment of the sugar moiety (397.0921, 379.0871, 361.0719 and 321.0764 *m/z*), so allowing to proposed an oxidation of the alcohol group contained in the aminosugar (see Figure S3 for the fragmentation pathways).

A TP with lower carbon content (530.1661 *m/z*, named **D-11**) was detected and attributed to demethylated doxorubicin. MS^2 spectrum showed as prominent ions 383.0769 *m/z*, due to the loss of the

sugar molecule and 365.0663 *m/z*, well matched with the most abundant ions formed in doxorubicin MS^2 spectrum minus a methyl group. The proposed fragmentation pathways are shown in Figure S4.

Additional transformation pathway involved the drug cleavage with the detachment of the aminosugar and the contemporaneous formation of **D-12** (413.0970 *m/z*) and **D-13** (148.0969 *m/z*), attributed to the hydroxyl-aminosugar. Looking closer at **D-12**, the MS^2 key ion at 377.0712 *m/z*, due to concerted loss of a water and glyoxal molecule, allowed to invoke an oxidation of the methanol group. The proposed fragmentation pathways are collected in Figure S5.

Analyzing TP **D-13**, it was slowly formed and, in the considered times, the curve showed a monotonic increase. The most abundant ion products at 130.0860 and 112.0752 *m/z* were formed through the loss of one (or two) water molecules (see Figure S6 for a tentative fragmentation pattern). A further hydroxylation occurred and led to **D-14** (164.0923 *m/*z), very slowly formed.

All characterized TPs allowed to hypothesize the different abiotic degradation processes to which doxorubicin is subjected once entered in water bodies and a tentative collection of transformation pathways is reported in Figure 6.

Based on the TPs temporal profiles, all the characterized compounds could be formed according to nine competitive pathways. The favourite transformation routes are those involving hydroxylation or demethylation for both photolysis and photocatalytic processes.

3.4. Characterization of methotrexate transformation products

The degradation of methotrexate through direct photolysis or in the presence of TiO_2 leads to the formation of TPs collected in Table 2. The isotopic abundance pattern was used as a powerful additional constraint for identification of these unknowns.

Along with the methotrexate degradation, seven TPs were identified under photolysis and eight TPs were formed under heterogeneous photocatalysis. These TPs followed a different kinetic profile depending on the diverse experimental conditions, as assessed by Figures S7 and S8. All TPs formed through an heterogeneous process were also identified in homogeneous photolysis, with the only exception of the species **M-8**. In both cases, **M-3** and **M-4** were the more abundant TPs and were easily formed, while **M-6**

and **M-7** were formed slowly and in a lower amount, reasonably due to the involvement of a multistep degradation pathway.

All the proposed structures are collected in Figure 7, where a tentative transformation route is proposed. Two pteridinic derivatives are known to be formed through a photolytic process [31] but were not identified in our studies.

Methotrexate underwent decarboxylation and hydroxylation with the formation of two species at 427.1837 *m/z* (named **M-1** and **M-2**) and empirical formula $C_{19}H_{23}N_8O_4$.

MS^2 and MS^3 study did not led to the identification of any peculiar product ions. However, reasonably both decarboxylation and hydroxylation were expected to involve the two carboxylic moieties and, based on their retention times, **M-1** should be attributed to the reduced form of the 5-carboxylic and **M-2** to the 1-carboxylic acid of glutamylamide.

Further molecule transformation involved the cleavage of the C-N bond with the formation of TPs at 281.1135 (**M-3**) and 209.0789 (**M-4**) *m/z*. The species **M-3**, with empirical formula $C_{13}H_{17}N_2O_5$, is attributed to N-[4-(methylamino)benzoyl]glutamic acid. Confirm arose from MS^2 study. The MS^2 fragmentation produced as base peak the ion at 134.0599 *m/z* though the loss of aminosuccinic acid. The absence of the key methotrexate product ion at 175.0659 *m/z* proved the detachment of the pteridinic moiety.

M-3 was further transformed into **M-5** following N-demethylation. MS^2 study evidenced the formation of a product ion at 120.0441 *m/z* (base peak) following the cleavage of the amide bond. A competitive cleavage of this bond could promote a shift of the hydroxyl group with the formation of the ion at 138.0548 *m/z* through a neutral loss (*para*-aminobenzoic acid). The formation of a product ion at 130.0497 *m/z* should be rationalized by assuming the protonation of the amidic nitrogen and the further loss of *para*-aminobenzoic acid (see Figure S9).

TP **M-4** with empirical formula $C_7H_9N_6O_2$ was attributed to the dihydroxylated pteridinic substructure of the drug.

Following the detachment of the alkyl chain, a TP at 179.0678 *m/z* (named **M-6**) and empirical formula $C_6H_7N_6O$ was formed. An alternative molecule cleavage led to the formation of a species with 163.0727 *m/z* (named **M-7**) and empirical formula $C_6H_7N_6$.

In addition to these shared intermediate compounds, addition of titanium dioxide started a supplementary transformation pathway, as a TP at 325.1520 *m/z* (**M-8**) and empirical formula $C_{15}H_{17}N_8O$ was detected; its empirical formula suggested the elimination of succinic acid from methotrexate.

All characterized TPs should be formed according to the four concomitant pathways shown in Scheme 5. Pathway **I** was the main transformation route and involved the drug cleavage with the formation of **M-3** and **M-4**, further transformed into **M-5** or **M-6** and **M-7**, respectively. A competitive pathway brings about **M-1** or **M-2** (see route **II** and **III**), while the addition of titanium dioxide starts a forth route (pathway **IV**).

3.5. Toxicity assessment

Acute toxicity was evaluated by monitoring changes in the natural emission of the luminescent bacteria *Vibrio fischeri* when challenged with toxic compounds and was expressed as percentage of inhibition of the bacteria luminescence. Results obtained on samples subjected to heterogeneous photocatalysis are plotted in Figure 8. By considering doxorubicin, the percentage of inhibition effect increased and reached the maximum after 15 min (43 % of inhibition) and then slowly decreased. This toxicity curve displays a shape similar to that followed by TPs (see Figure 3), as for most TPs maxima concentration was obtained after 15 min of irradiation.

Looking closer to methotrexate, the toxicity was kept at maximum level until 30 min of irradiation and then decreased until 2h of irradiation, where it was very low (10% of inhibition). Biotransformation of methotrexate is known to form 7-hydroxy methotrexate, an highly toxic compound, not detected in our experimental conditions [21]. The disappearance of the methotrexate is already complete after 10 minutes, so that the observed high toxicity till 30 min has to be attributed to its TPs. At longer irradiation times (45 min) there is a severe reduction of the toxicity to 40%, further reduced at longer irradiation times. Some initial TPs, i.e. species **M-1**, **M-3** and **M-5** should justifying the high relative toxicity up to times of irradiation of 15 minutes, while other transformation products, i.e. species **M-4**, **M-6** and **M-7**, are still present in longer exposure time, justifying the persistence of a slight toxicity. Thus, even if ultimate TPs still showed a certain toxicity, the more toxic compounds seemed to be those formed during the initial steps of drug transformation.

4. Conclusions

The study of doxorubicin and methotrexate transformations through photolysis and photocatalyzed degradation process, using titanium dioxide as a photocatalyst, was investigated. Methotrexate underwent degradation both under UV-A irradiation and heterogeneous photocatalytic treatment, while doxorubicin looks rather stable under UV-a irradiation. LC-HRMS permitted to identify and characterized fourteen and eight TPs from doxorubicin and methotrexate degradation, respectively.

This study evidences that high resolution mass spectrometry, combined with LC, is a technique able to play a key role in the evaluation of the potential environmental fate of pollutants and permitted to recognize the photocatalytic transformation pathways followed by the two drugs. The new compounds identified in this way will be sought in future environmental investigations to extend the range of detection of pharmaceutical pollutants.

References

[1] C.G. Daughton, Emerging Pollutants and Communicating the Science of Environmental Chemistry and Mass Spectrometry- Pharmaceuticals in the Environment, J. Am. Soc. Mass Spectrom. 12 (10) (2011) 1067-1076.

[2] S.K. Khetan, T.J. Collins, Human Pharmaceuticals in the environment: a challenge to green chemistry, Chem. Rev., 107(6) (2007) 2319-2364

[3] E. Zuccato, S. Castiglioni, R. Bagnati, M. Melis, R. J. Fanelli, Source, occurrence and fate of antibiotics in the Italian aquatic environment, Hazard. Mater. 179(2) (2010) 1042-1048

[4] P. Vasquez-Roig, C. Blasco, Y. Picò, Advances in the analysis of legal and illegal drugs in the aquatic environment, TrAC Trends in Analytical Chemistry, 50 (2013) 65-77

[5] T. Kosjek, E. Heath, Occurrence, fate and determination of cytostatic pharmaceuticals in the environment, TrAC-Trends Anal. Chem., 30(7) (2011) 1065-1087

[6] L. Kovalona, C.S. McArdell, J. Hollander, Challenge of high polarity and low concentrations in analysis of cytostatics and metabolites in wastewater by hydrophilic interaction chromatography/tandem mass spectrometry, J. Chromatogr. A 1216 (2009) 1100-1108

[7] S. Castiglioni, R. Bagnati, D. Calamari, R. Fanelli, E. Zuccato, A multiresidue analytical method using solid-phase extraction and high-pressure liquid chromatography tandem mass spectrometry to measure pharmaceuticals of different therapeutic classes in urban wastewaters, J. Chromatogr. A 1092 (2005) 206-215.

[8] T.A. Ternes, R. Hirsch, J. Mueller, Methods for the determination of neutral drugs as well as betablockers and beta(2)-sympathomimetics in aqueous matrices using GC/MS and LC/MS/MS, Fresenius J. Anal. Chem. 362 (1998) 329-340.

[9] T.A. Ternes, M. Bonerz, N. Herrmann, D. Loffler, E. Keller, B. Bago Lacida, A.C. Alder, Determination of pharmaceuticals, iodinated contrast media and musk fragrances in sludge by LC/tandem MS and GC/MS, J. Chromatogr. A 1067 (2005) 213-223.

[10 N. Negreira, N. Mastroianni, M. Lòpez de Alda, D. Barcelò, Multianalyte determination of 24 cytostatics and metabolites by liquid chromatography–electrospray–tandem mass spectrometry and study of their stability and optimum storage conditions in aqueous solution, Talanta 116 (2013) 290-299

[11] L. Ferrando-Climent, S. Rodriguez-Mozaz, D. Barcelo, Development of a UPLC-MS/MS method for the determination of ten anticancer drugs in hospital and urban wastewaters, and its application for the screening of human metabolites assisted by information-dependent acquisition tool (IDA) in sewage samples, Anal. Bioanal. Chem. 405 (18) (2013) 5937-5952

[12] I. Ferrer, E.M. Thurman, Analysis of pharmaceuticals in drinking water, groundwater, surface water, and wastewater, Comprehensive Analytical Chemistry, 62 (2013) 91-128.

[13] A. Pérez-Parada, A. Agüera, M. Del Mar Gómez-Ramos, J.F. García-Reyes, H. Heinzen, A.R. Fernández-Alba, Behavior of amoxicillin in wastewater and river water: Identification of its main transformation products by liquid chromatography/electrospray quadrupole time-of-flight mass spectrometry, Rapid Comm. Mass Spectrom., 25 (6) (2011) 731-742.

[14] N.Tokman, C. Soler, l Farré, Marinel. Y. Picó, D. Barceló, Determination of amitraz and its transformation products in pears by ethyl acetate extraction and liquid chromatography-tandem mass spectrometry, J. Chromat. A, 1216 (15) (2009) 3138-3146.

[15] W.F. Smyth, Recent studies on the electrospray ionisation mass spectrometric behaviour of selected nitrogen-containing drug molecules and its application to drug analysis using liquid chromatography-electrospray ionisation mass spectrometry, J. Chromat. B: Analytical Technologies in the Biomedical and Life Sciences, 824 (1-2) (2005) 1-20.

[16] C. Medana, P. Calza, F. Dal Bello, E. Raso, C. Minero, C. Baiocchi, Multiple unknown degradants generated from the insect repellent DEET by photoinduced processes on TiO_2, J. Mass Spectrometry 46 (2011) 24-40

[17] J. Yin, B. Shao, J. Zhang, K. Li, Bull. Environ. Contam. Toxicol. 84 (2010) 39.

[18] C. Medana, P. Calza, F. Dal Bello, C. Baiocchi, LC-HRMS determination of anti-cancer drugs as occupational contaminants applied to photocatalytic degradation of molecules of different stability, LC GC North Am. S (2013) 38-45

[[19] S.N. Mahnik, B. Rizovski, M. Fuerhacker, R.M. Mader, Development of an analytical method for the determination of anthracyclines in hospital effluents, Chemosphere 65 (2006) 1419-1425.

[20] G.W. Aherne, J. English, V. Marks, The role of immunoassay in the analysis of microcontaminants in water samples, Ecotoxicol. Environ. Saf. 9 (1985) 79-83.

[21] T. Kiffmeyer, H.J. Gotze, M. Jursch, U. Luders, Trace enrichment, chromatographic separation and biodegradation of cytostatic compounds in surface water Fresenius J. Anal. Chem., 361 (1998) 185-191

[22] TOXNET: Hazardous Substances Data Bank (HSDB), [Online] U.S. National Library of Medicine (http://toxnet.nlm.nih.gov/cgi-bin/sis/htmlgen?HSDB) (accessed in February 2011).

[23] S.N. Mahnik, K. Lenz, N. Weissenbacher, R.M. Mader, M. Fuerhacker, Fate of 5-fluorouracil, doxorubicin, epirubicin, and daunorubicin in hospital wastewater and their elimination by activated sludge and treatment in a membrane-bio-reactor system, Chemosphere 66 (2007) 30-37

[24] T. Ohno, K. Sarukawa, K. Tokieda, M. Matsumura, Morphology of a TiO_2 photocatalyst (Degussa, P-25) consisting of anatase and rutile crystalline phases, J. Catal. 203 (2001) 82-86

[25] A. Mills, S. Le Hunte, An overview of semiconductor photocatalysis, J. Photochem. Photobiol. A: Chem. 108 (1997) 1-35

[26] D. Robert, S. Malato, Solar photocatalysis: a clean process for water detoxification, Sci. Total Environ. 291 (2002) 85-97

[27] M. R. Hoffmann, S. T. Martin, W. Choi, D.W. Bahnemann, Environmental Applications of Semiconductor Photocatalysis, Chem. Rev. 95 (1995) 69-96

[28] P. Calza, C. Medana, E. Raso, V. Gianotti, C. Minero, N,N-diethyl-m-toluamide transformations in river water, Sci. Tot. Environ. 409 (2011) 3894-3901

[29] P. Calza, C. Medana, E. Padovano, V. Giancotti, C. Minero, Fate of selected pharmaceuticals in River waters, Environ. Sci. Pollut. Res. 20(4) (2013) 2262-2270

[30] P. Calza, S. Marchisio, C. Medana, C. Baiocchi, Fate of the antibacterial spiramycin in river waters, Anal. Bioanal. Chem. 396(4) (2010) 1539–1550

[31] C. Chahidi, M. Giraud, M. Aubailly, A. Valla, R. Santus, 2,4-diamini-6-pteridinecarboxaldehyde and an azobenzene derivative are produced by UV photodegradation of methotrexate, Photochem. Photobiol. 44(2) (1986) 231-233

Figure captions

Figure 1. Degradation of doxorubicin 15 mg L^{-1} (top) and methotrexate (bottom) as a function of irradiation time in ultrapure water or ultrapure water spiked with TiO_2 (200 mg L^{-1}).

Figure 2. Doxorubicin and methotrexate proposed fragmentation pathways.

Figure 3. Transformation products formed from doxorubicin degradation plotted as a function of the irradiation time in the presence of 200 mg/L TiO_2

Figure 4. LC-ESI HRMS chromatogram of **D-1** and **D-2** degradation products after 5 min of irradiation, together with the key fragmentation pathways.

Figure 5. MS^2 spectra of degradation products **D-3** (top), **D-4** (middle) and **D-5** (bottom) together with the proposed fragment ions.

Figure 6. Proposed transformation pathways followed by doxorubicin under irradiation.

Figure 7. Transformation pathways followed by methotrexate under irradiation.

Figure 8. Inhibition (%) of the luminescence of bacteria *Vibrio fischeri* for doxorubicin (top) and methotrexate (bottom) as a function of the irradiation time.

Scheme 1. Doxorubicin MH^+ MS^2 proposed fragmentation pathways.

Scheme 2. Methotrexate MS^2 and MS^3 proposed fragmentation pathways**.**

Scheme 3. Proposed transformation pathways followed by doxorubicin under irradiation.

Scheme 4. Proposed fragmentation pathways for M-5.

Scheme 5. Transformation pathways followed by methotrexate under irradiation.

Scheme 1

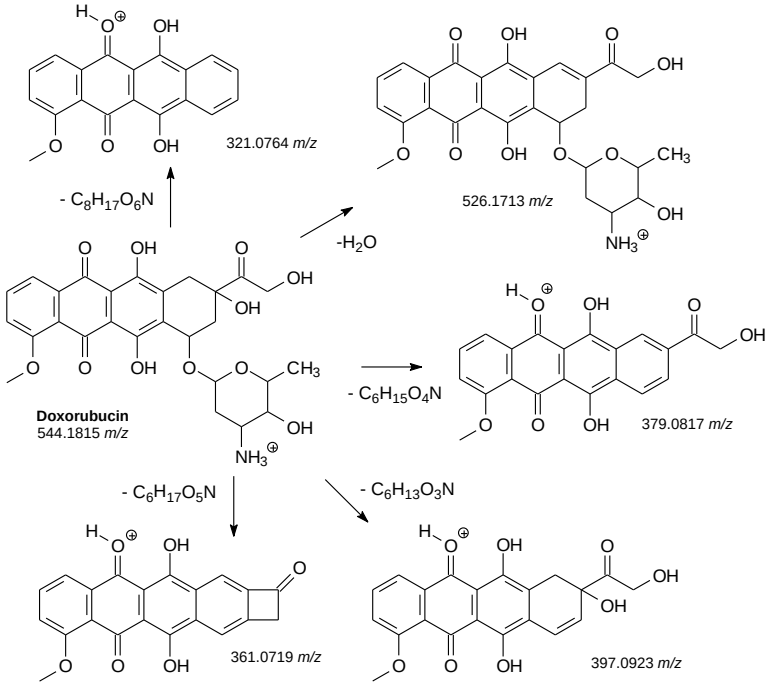
321.0764 m/z
- C8H17O6N
-H2O
526.1713 m/z
Doxorubucin
544.1815 m/z
- C6H15O4N
379.0817 m/z
- C6H17O5N
- C6H13O3N
361.0719 m/z
397.0923 m/z

Scheme 2.

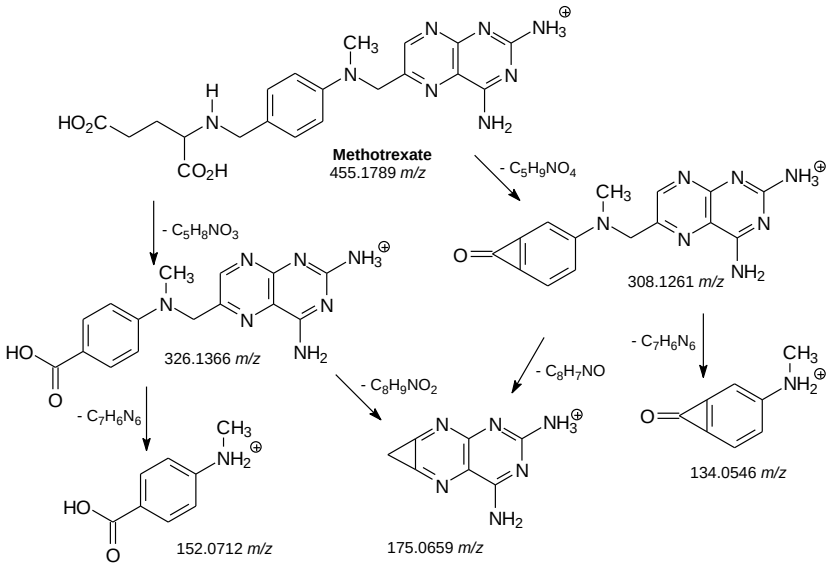
Methotrexate
455.1789 m/z
- C5H9NO4
308.1261 m/z
- C5H8NO3
326.1366 m/z
- C7H6N6
152.0712 m/z
- C8H9NO2
175.0659 m/z
- C8H7NO
- C7H6N6
134.0546 m/z

Scheme 3

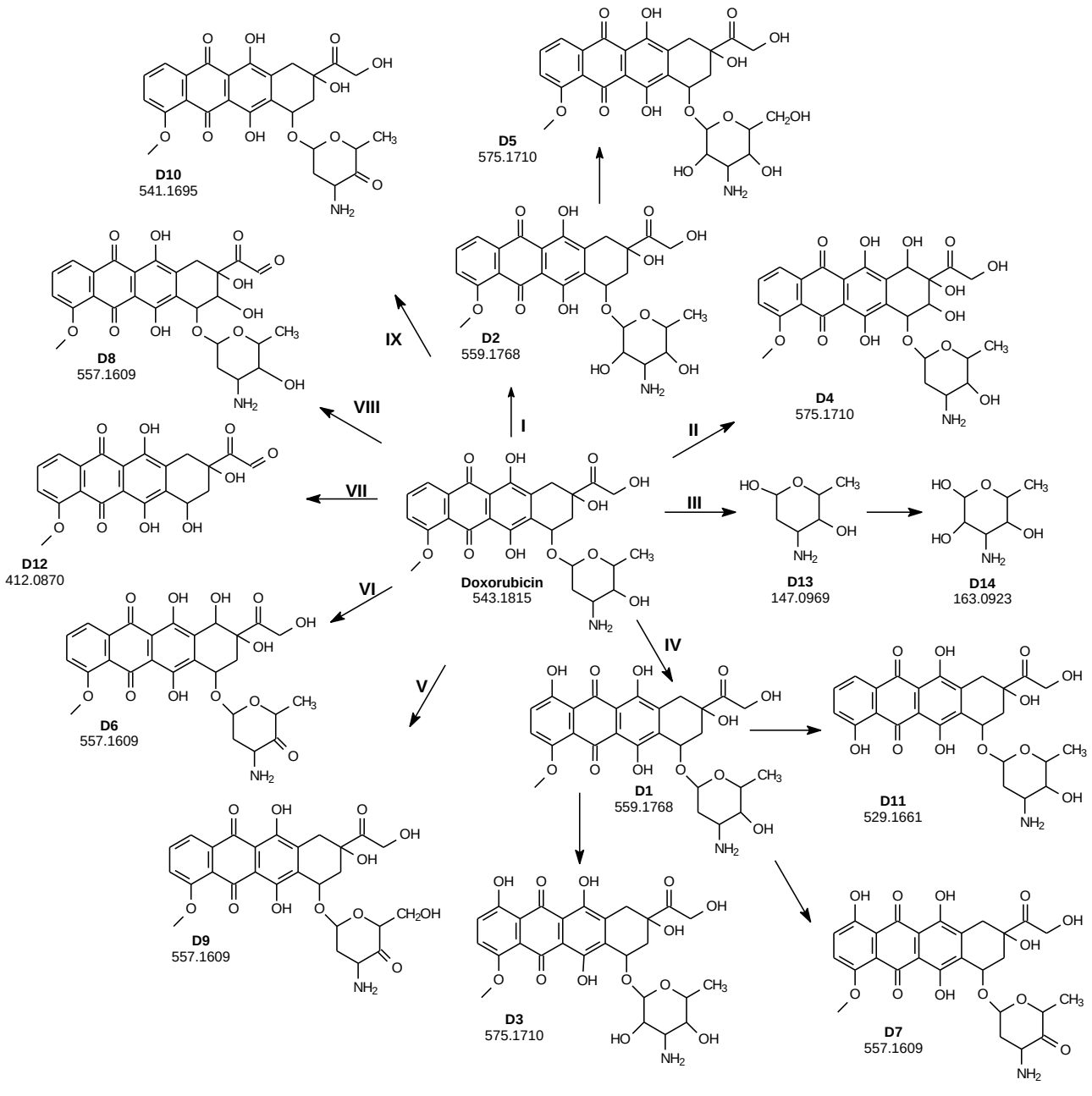
D10
541.1695
D5
575.1710
D8
557.1609
D2
559.1768
D4
575.1710
IX
VIII
I
II
D12
412.0870
VII
Doxorubicin
543.1815
III
D13
147.0969
D14
163.0923
VI
IV
V
D6
557.1609
D1
559.1768
D11
529.1661
D9
557.1609
D3
575.1710
D7
557.1609

Scheme 4

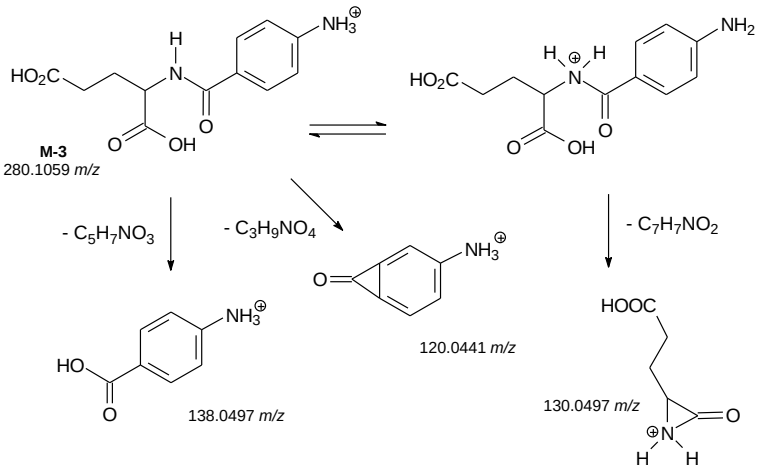
M-3
280.1059 m/z
- C5H7NO3
- C3H9NO4
- C7H7NO2
138.0497 m/z
120.0441 m/z
130.0497 m/z

Scheme 5

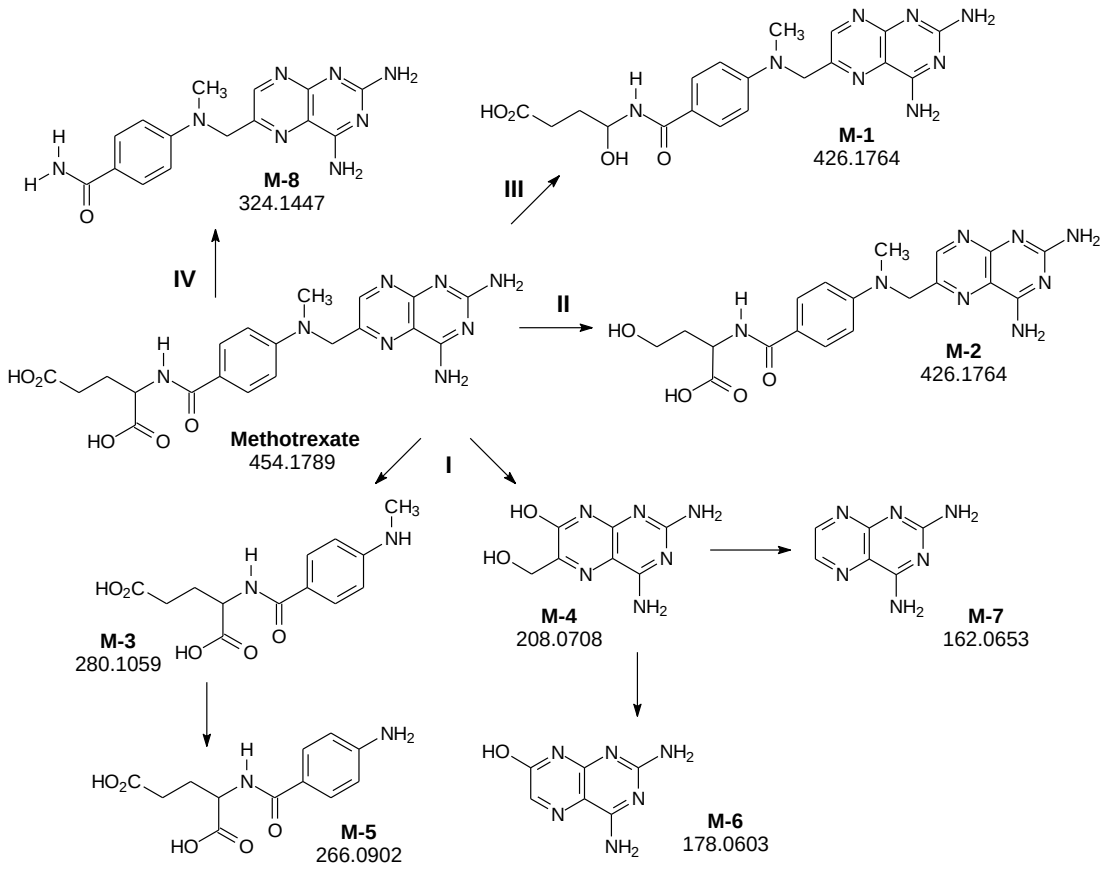

Figure 1

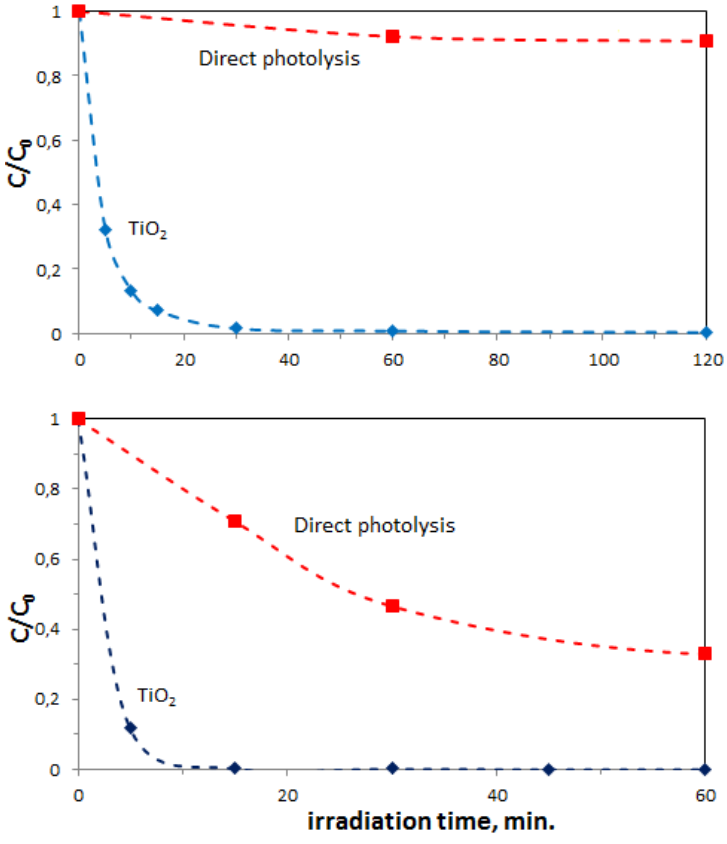
1
0,8
0,6
0,4
0,2
0
C/C0
Direct photolysis
TiO2
0
20
40
60
80
100
120
1
0,8
0,6
0,4
0,2
0
C/C0
Direct photolysis
TiO2
0
20
40
60
irradiation time, min.

Figure 2

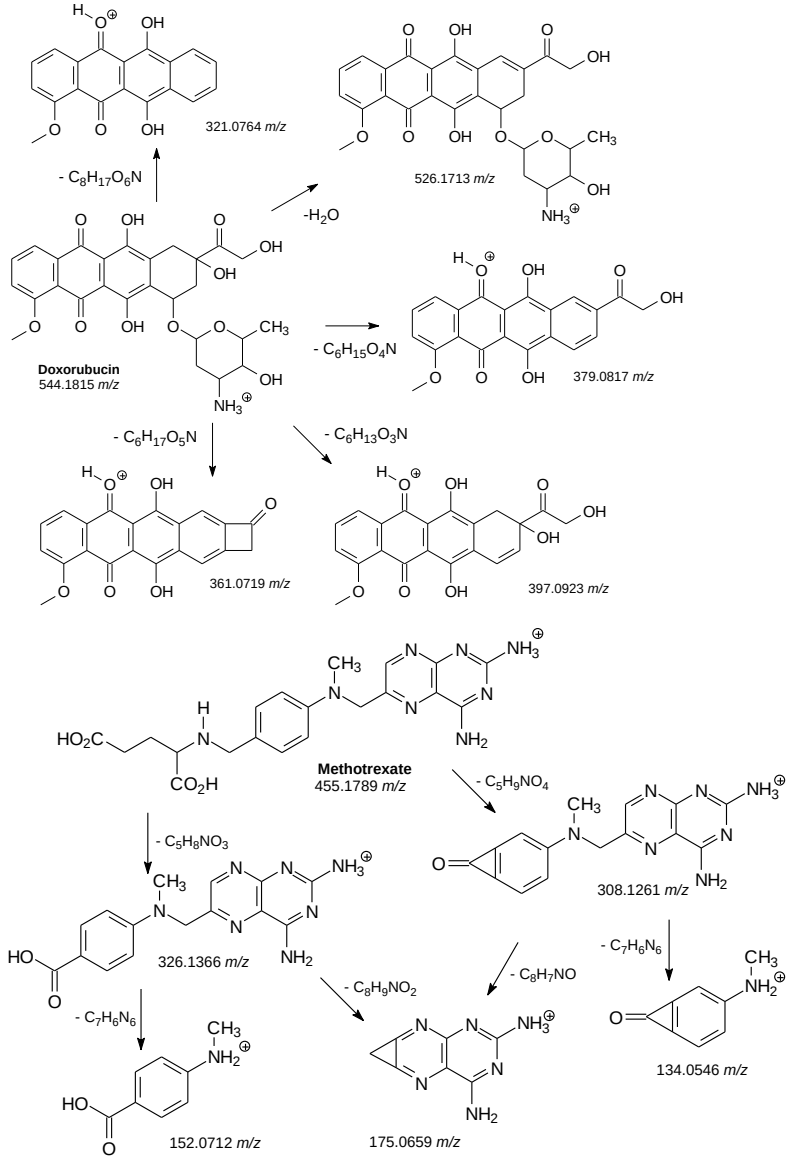
321.0764 m/z
526.1713 m/z
- C8H17O6N
-H2O
Doxorubucin
544.1815 m/z
- C6H15O4N
379.0817 m/z
- C6H17O5N
- C6H13O3N
361.0719 m/z
397.0923 m/z
Methotrexate
455.1789 m/z
- C5H9NO4
- C5H8NO3
308.1261 m/z
326.1366 m/z
- C7H6N6
- C8H7NO
- C8H9NO2
134.0546 m/z
152.0712 m/z
175.0659 m/z

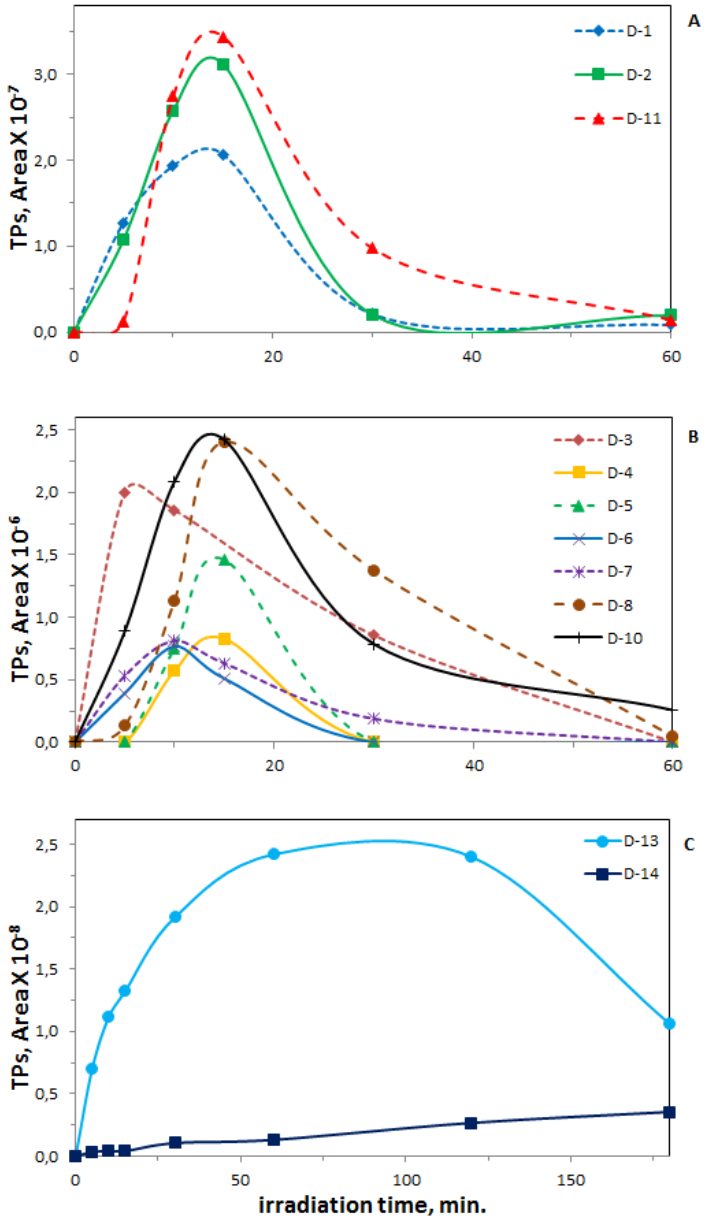
A
D-1
D-2
D-11
TPs, Area X 10-7
3,0
2,0
1,0
0,0
0
20
40
60
B
D-3
D-4
D-5
D-6
D-7
D-8
D-10
TPs, Area X 10-6
2,5
2,0
1,5
1,0
0,5
0,0
0
20
40
60
C
D-13
D-14
TPs, Area X 10-8
2,5
2,0
1,5
1,0
0,5
0,0
0
50
100
150
irradiation time, min.

Figure 3

Figure 4

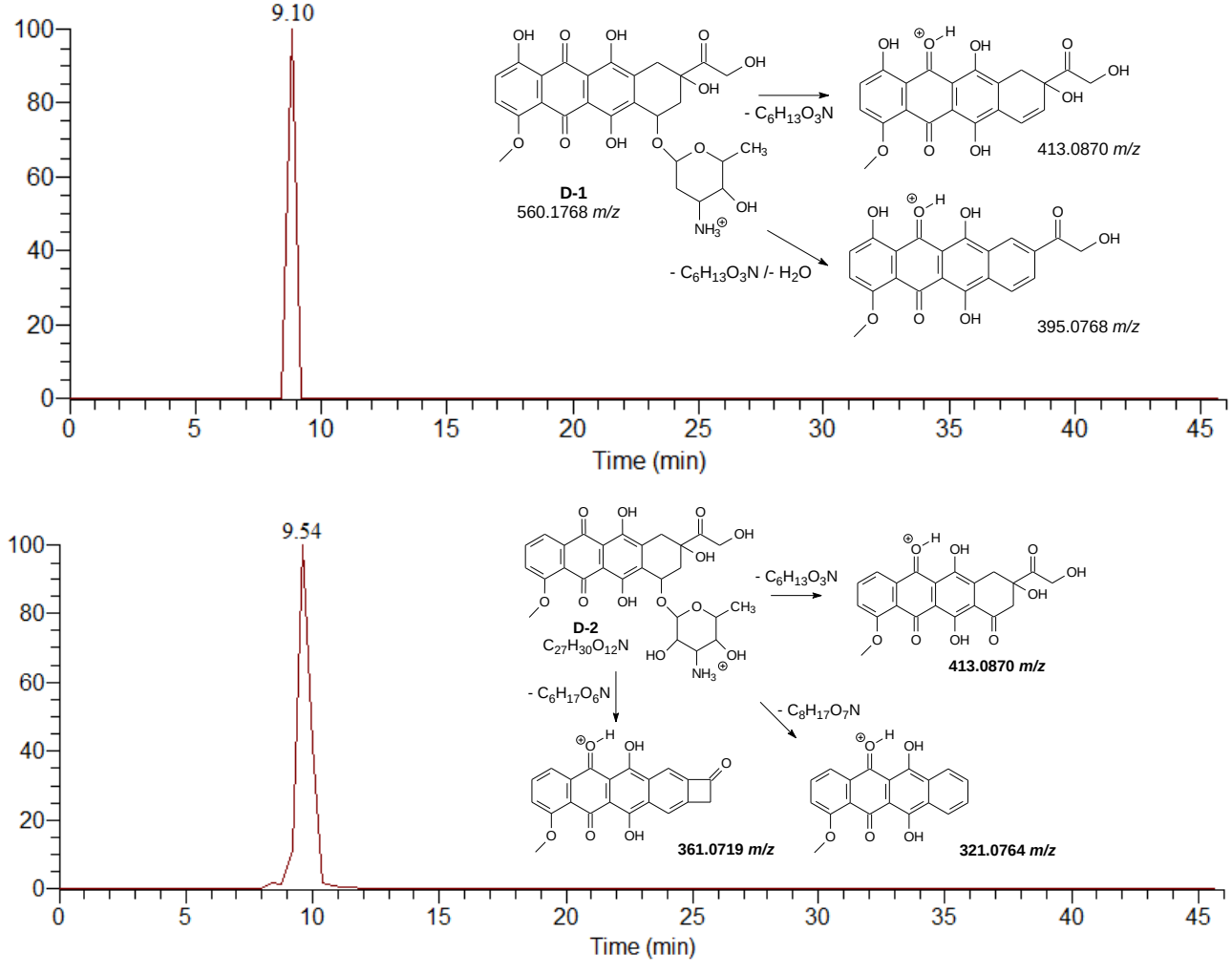
9.10
100
80
60
40
20
0
0
5
10
15
20
25
30
35
40
45
Time (min)
D-1
560.1768 m/z
- C6H13O3N
413.0870 m/z
- C6H13O3N /- H2O
395.0768 m/z
9.54
D-2
C27H30O12N
- C6H13O3N
413.0870 m/z
- C6H17O6N
361.0719 m/z
- C8H17O7N
321.0764 m/z

Figure 5

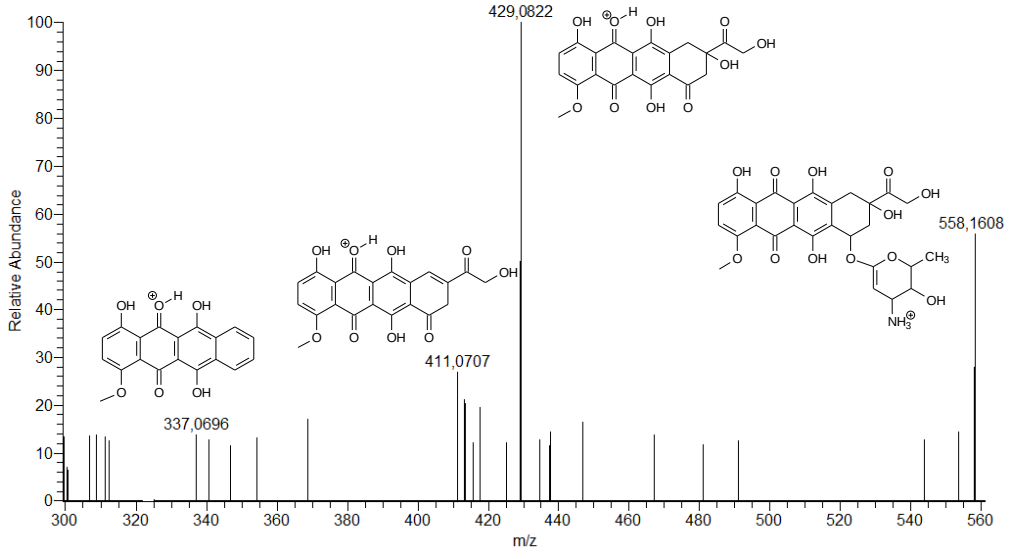
429,0822
558,1608
411,0707
337,0696
Relative Abundance
m/z

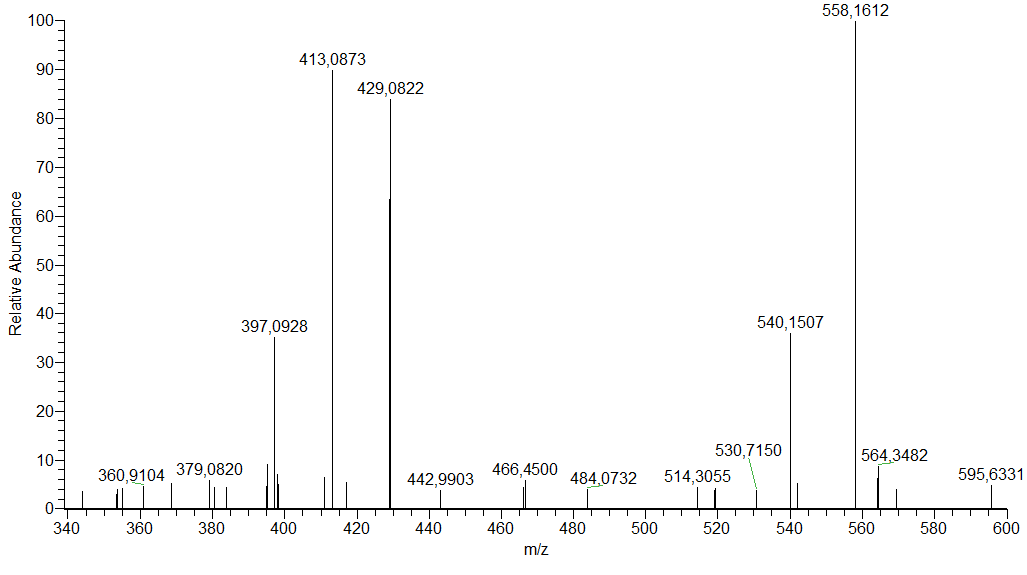
558,1612
413,0873
429,0822
397,0928
540,1507
530,7150
564,3482
595,6331
360,9104
379,0820
442,9903
466,4500
484,0732
514,3055
Relative Abundance
m/z

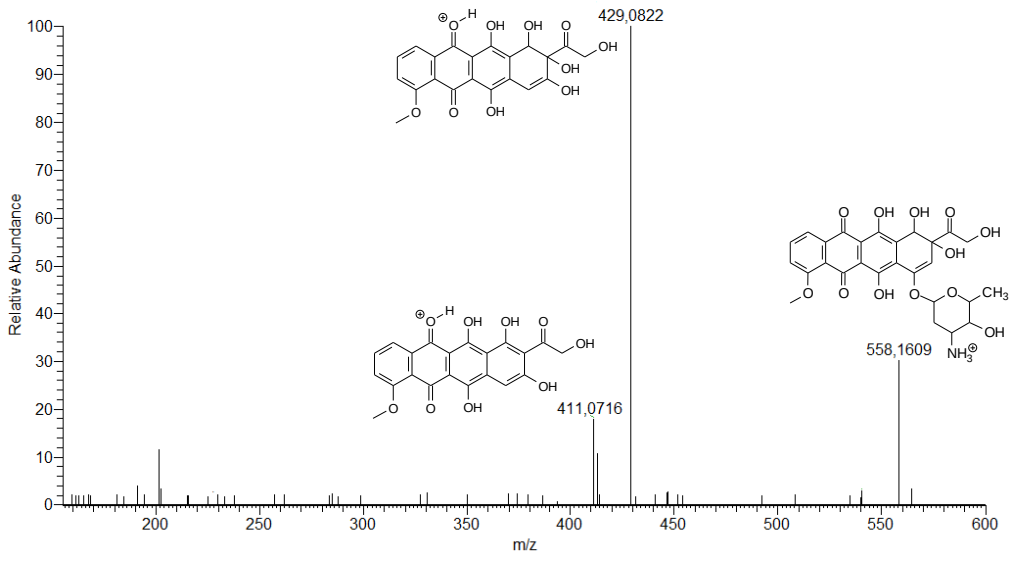
429,0822
411,0716
558,1609
Relative Abundance
m/z

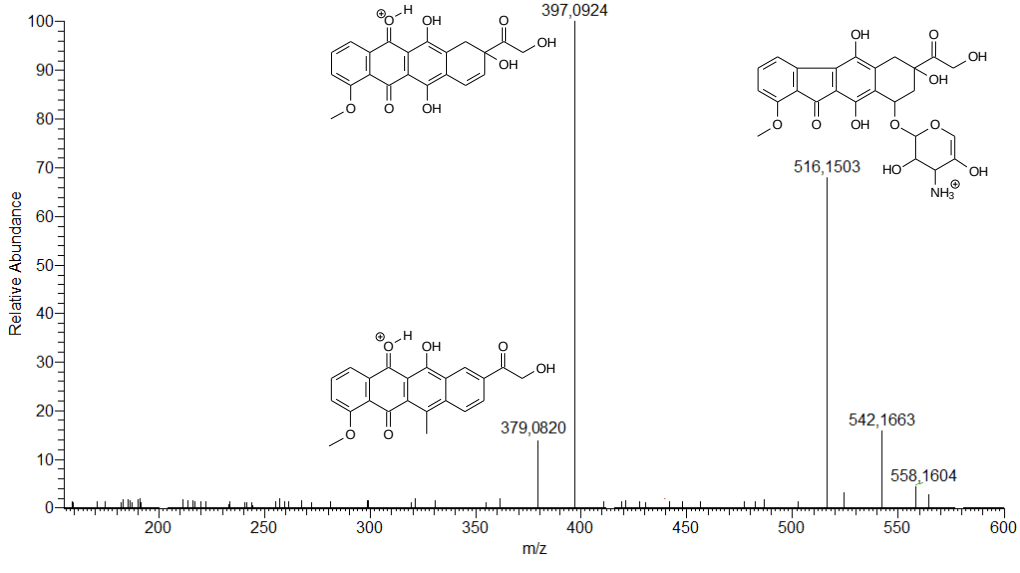
397,0924
516,1503
379,0820
542,1663
558,1604
Relative Abundance
m/z

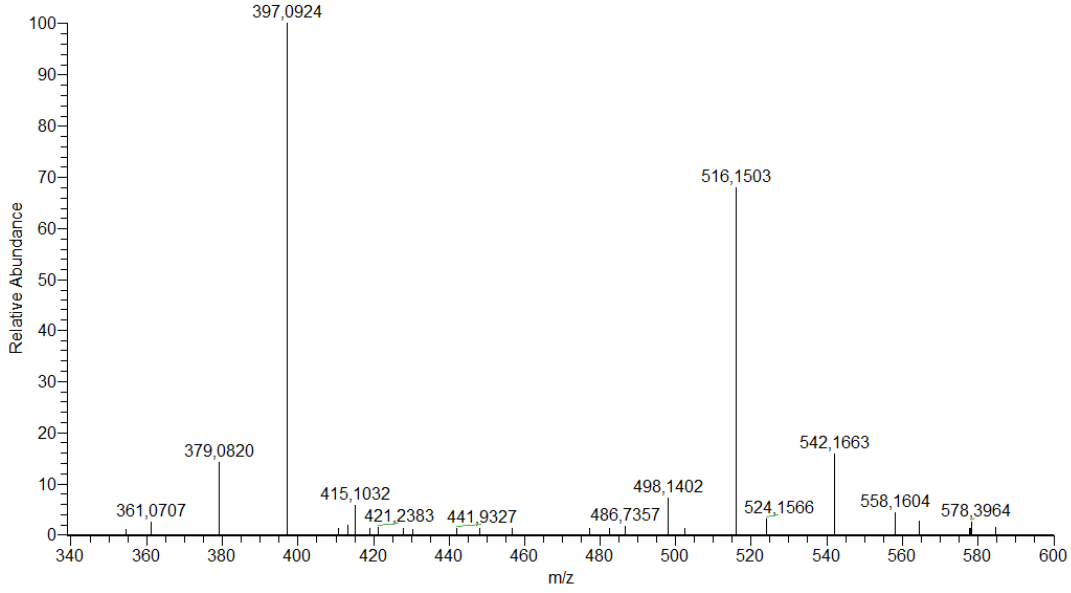
397,0924
516,1503
379,0820
542,1663
415,1032
498,1402
361,0707
421,2383
441,9327
486,7357
524,1566
558,1604
578,3964
Relative Abundance
m/z
100
90
80
70
60
50
40
30
20
10
0
340
360
380
400
420
440
460
480
500
520
540
560
580
600

Figure 6

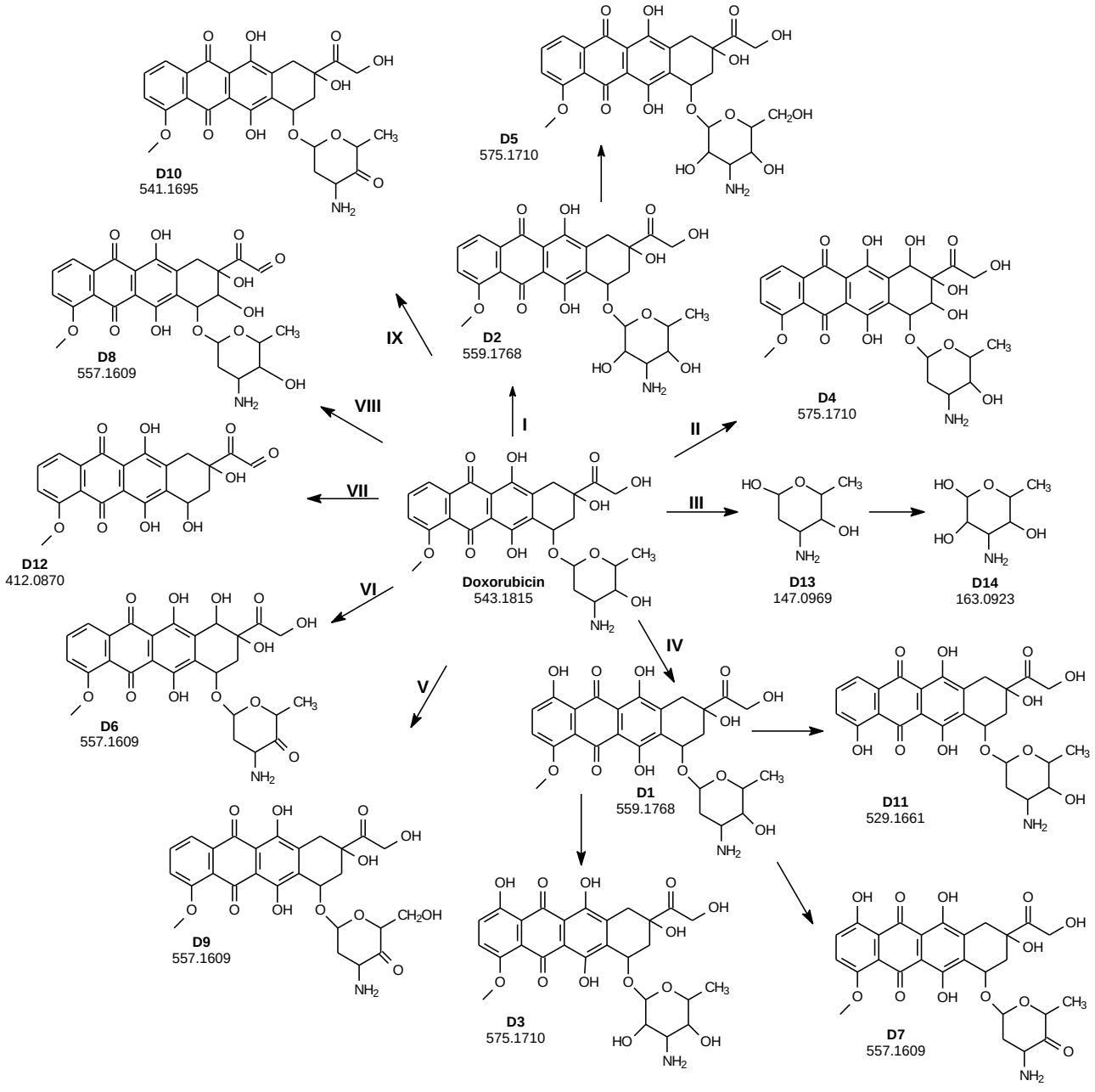
D10
541.1695
D5
575.1710
D8
557.1609
D2
559.1768
D4
575.1710
D12
412.0870
Doxorubicin
543.1815
D13
147.0969
D14
163.0923
D6
557.1609
D1
559.1768
D11
529.1661
D9
557.1609
D3
575.1710
D7
557.1609
I
II
III
IV
V
VI
VII
VIII
IX

figure 7

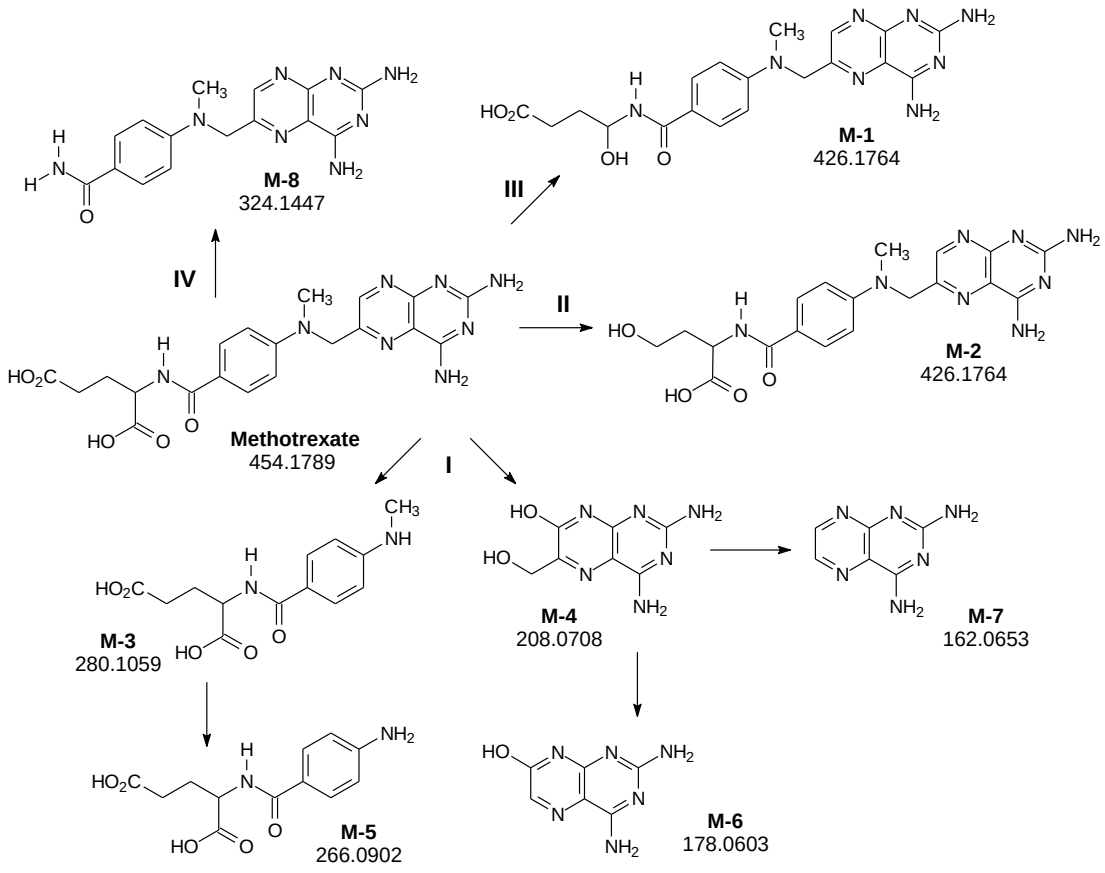
M-8
324.1447
M-1
426.1764
III
IV
II
M-2
426.1764
Methotrexate
454.1789
I
M-3
280.1059
M-4
208.0708
M-7
162.0653
M-5
266.0902
M-6
178.0603

Figure 8

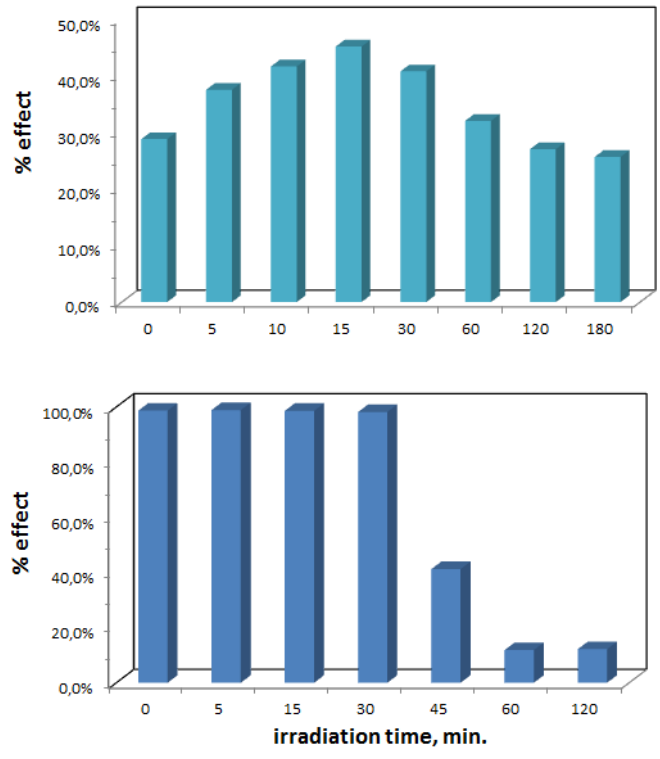
50,0%
40,0%
30,0%
20,0%
10,0%
0,0%
% effect
0
5
10
15
30
60
120
180
100,0%
80,0%
60,0%
40,0%
20,0%
0,0%
% effect
0
5
15
30
45
60
120
irradiation time, min.